Hindawi
Science and Technology of Nuclear Installations
Volume 2018, Article ID 7635878, 19 pages
https://doi.org/10.1155/2018/7635878

Research Article

ROSA/LSTF Tests and Posttest Analyses by RELAP5 Code for Accident Management Measures during PWR Station Blackout Transient with Loss of Primary Coolant and Gas Inflow

Takeshi Takeda [1,2] **and Iwao Ohtsu** [2]

[1] *Nuclear Regulation Authority, 1-9-9 Roppongi, Minato-ku, Tokyo-to 106-8450, Japan*
[2] *Japan Atomic Energy Agency, 2-4 Shirakata-Shirane, Tokai-mura, Naka-gun, Ibaraki-ken 319-1195, Japan*

Correspondence should be addressed to Takeshi Takeda; takeda.takeshi4695@gmail.com

Received 29 March 2018; Accepted 20 July 2018; Published 2 September 2018

Academic Editor: Stephen M. Bajorek

Three tests were carried out with the ROSA/LSTF (rig of safety assessment/large-scale test facility), which simulated accident management (AM) measures during station blackout transient with loss of primary coolant under assumptions of nitrogen gas inflow and total failure of high-pressure injection system in a pressurized water reactor. As the AM measures, steam generator (SG) secondary-side depressurization was done by fully opening the relief valves in both SGs, and auxiliary feedwater was injected into the secondary-side of both SGs simultaneously. Conditions for the break size and the onset timing of the AM measures were different among the three LSTF tests. In the three LSTF tests, the primary pressure decreased to a certain low pressure of below 1 MPa with or without the primary depressurization by fully opening the relief valve in a pressurizer as an optional AM measure, while no core uncovery took place through the whole transient. Nonuniform flow behaviors were observed in the SG U-tubes under natural circulation (NC) with nitrogen gas depending probably on the gas accumulation rate in the two LSTF tests that the gas accumulated remarkably. The RELAP5/MOD3.3 code predicted most of the overall trends of the major thermal hydraulic responses observed in the three LSTF tests. The code, however, indicated remaining problems in the predictions of the primary pressure, the SG U-tube collapsed liquid levels, and the NC mass flow rate after the nitrogen gas ingress as well as the accumulator flow rate through the analyses for the two LSTF tests, where the remarkable gas accumulation occurred.

1. Introduction

In the earthquake and tsunami-induced station blackout (SBO) accident at the Fukushima Daiichi boiling water reactor, water was alternatively injected into the reactor as a flexible applied action utilizing fire engines due to loss of the core cooling functions [1]. The effectiveness of accident management (AM) measures should be considered for long-term core cooling under conditions of severe multiple system failures similar to the Fukushima Daiichi accident. Steam generator (SG) secondary-side depressurization through the SG valve(s) is one of major AM measures to cool and depressurize the primary system via natural circulation (NC) because of steam condensation in the SG U-tubes especially when high-pressure injection system of emergency core cooling system (ECCS) is totally failed during accidents and transients in a pressurized water reactor (PWR). Several studies [2–6] have been conducted to investigate thermal hydraulic responses in SBO scenarios with AM measures of PWRs by calculations with best-estimate computer codes. Some researchers [7, 8] have analyzed loss of primary coolant and SBO events in PWRs employing severe accident computer codes, but under the condition modeling for the pressure vessel internals except the core and the downcomer was more simplified than that in the best-estimate computer codes. Meanwhile, there have been some experimental researches on the PWR SBO scenarios with AM measures by using such integral test facilities as the PSB for VVER in Russia [9]

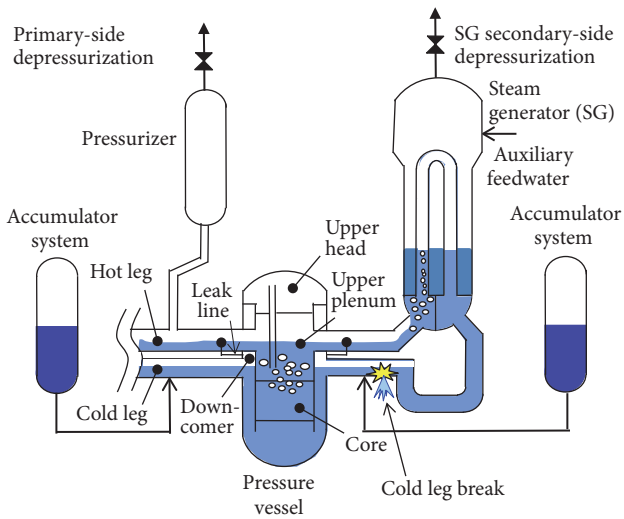

Figure 1: Coolant behavior during SBO transient with loss of primary coolant and AM measure [11].

and the PKL for Vorkonvoi-type PWR in Germany [10]. The experimental data, however, would be insufficient to clarify the AM measures effectiveness due to such atypical features as small volume and low pressure in the primary system.

Yoshihara [12] has put forward that accumulator (ACC) system of ECCS should be isolated by the closure of motor-operated valves located at the outlet of ACC tanks utilizing emergency power generators when the primary pressure decreases to a certain low pressure during PWR SBO transient with leakage from primary coolant pump seal. This prevents noncondensable gas (nitrogen gas) used for pressurization of ACC tanks from entering the primary system. If the isolation of ACC system is failed after the coolant injection initiation, ingress of nitrogen gas to the primary system takes place following the completion of ACC coolant injection, suggesting that degradation in the condensation heat transfer in the SG U-tubes should affect the core cooling [13, 14]. The nitrogen gas enters cold legs through ECCS nozzles first and then migrates to hot legs through the vessel downcomer and hot leg leak simulating lines that connect the downcomer to the hot legs, as shown in Figure 1. The nitrogen gas in the downcomer may flow into the vessel upper head. The nitrogen gas from the hot legs and the SG inlet plena accumulates in the SG U-tubes.

We [11, 15] have performed two simulation tests on AM measures during PWR SBO transient with or without the pump seal leakage (simulated by 0.1% cold leg break) [16] utilizing the large-scale test facility (LSTF) [17] in the rig of safety assessment (ROSA) program at Japan Atomic Energy Agency. The LSTF simulates a Westinghouse-type four-loop 3423 MW (thermal) PWR by a full-height and 1/48 volumetrically scaled two-loop system. The two LSTF tests assumed nitrogen gas inflow and total failure of high-pressure injection system regarding the severe multiple system failures. We considered the AM measures to depressurize SG secondary-side system by fully opening the safety valves in both SGs with the start of core uncovery first and then to inject coolant into the secondary-side of both SGs at low pressures taking the availability of fire engines into account. However, there were scarcely experimental data to understand the degradation in the primary depressurization due to nitrogen gas ingress under the NC when the primary pressure decreases to below 1 MPa assuming the use of systems relying on the low-head pumps.

In this study, we carried out three tests with the LSTF simulating AM measures during PWR SBO transient with loss of primary coolant under assumptions of nitrogen gas inflow and totally failed high-pressure injection system concerning the severe multiple system failures in 2015–2017. This study focused on nitrogen gas behavior during the NC when the primary pressure decreases to below 1 MPa. As the AM measures, we considered that the SG secondary-side depressurization was done by fully opening the relief valves in both SGs, and auxiliary feedwater (AFW) was injected into the secondary-side of both SGs by utilizing the turbine-driven pump at the same time. Table 1 shows the major test conditions. Conditions for the break size and the onset timing of the AM measures were different among the three LSTF tests. In a test denoted as TR-LF-18, the AM measures were initiated 10 min after 0.5% cold leg break. In a test denoted as TR-LF-17, the AM measures were started 20 min after 0.2% cold leg break. The conditions for the two tests were defined based on the small-break size and the delay of the operator's AM actions. In a test denoted as TR-LF-16, the AM measures were initiated simultaneously with 0.1% cold leg break, taking account of the pump seal leakage and the safety assurance measures by the PWR electric utilities in Japan [12]. We compared the results of the three LSTF tests mutually to make clear the influences of the break size and the onset timing of the AM measures. We analyzed further the three LSTF tests by using RELAP5/MOD3.3 code [18] to clarify the remaining subjects. This paper is concerned with the major results from the three LSTF tests and the posttest analyses with the RELAP5 code.

2. ROSA/LSTF

The ROSA/LSTF simulates a Westinghouse-type four-loop 3423 MW (thermal) PWR using a two-loop system model with full-height and 1/48 in volume. The reference PWR is Tsuruga Unit-2 of Japan Atomic Power Company.

Figure 2 shows the schematic view of the LSTF that is composed of a pressure vessel, pressurizer (PZR), and primary loops. Each loop includes an active SG, primary coolant pump, and hot and cold legs. Loops with and without PZR are designated as loop A and loop B, respectively. Each SG is furnished with 141 full-size U-tubes (inner diameter of 19.6 mm, nine different lengths as shown in Table 2), inlet and outlet plena, boiler section, steam separator, steam dome, steam dryer, main steam line, four downcomer pipes, and other internals. Six U-tubes are instrumented for each SG. Instrumented tubes designated as tubes 1 and 6 are short tubes (type 1 in Table 2), tubes 2 and 5 are medium tubes (type 5), and tubes 3 and 4 are long tubes (type 9). The hot and cold legs of 207 mm in inner diameter are sized to conserve

Table 1: Major conditions of LSTF tests.

Item	Condition		
	TR-LF-18	TR-LF-17	TR-LF-16
Break size	0.5%	0.2%	0.1%
Break location	Side of cold leg		Top of cold leg
Break valve open	Time zero		
High-pressure injection system	Total-failure		
Onset of SG secondary-side depressurization by fully opening relief valves in both SGs	10 min after break	20 min after break	Time zero
Onset of AFW injection into secondary-side of both SGs	Concurrent with SG secondary-side depressurization		

Table 2: Details of LSTF U-tubes in each SG.

Type	Straight length (m)	Number of tubes	Instrumented tubes
1	9.44	21	Two short tubes
2	9.59	19	
3	9.74	19	
4	9.89	19	
5	10.04	17	Two medium tubes
6	10.19	15	
7	10.34	13	
8	10.49	11	
9	10.64	7	Two long tubes

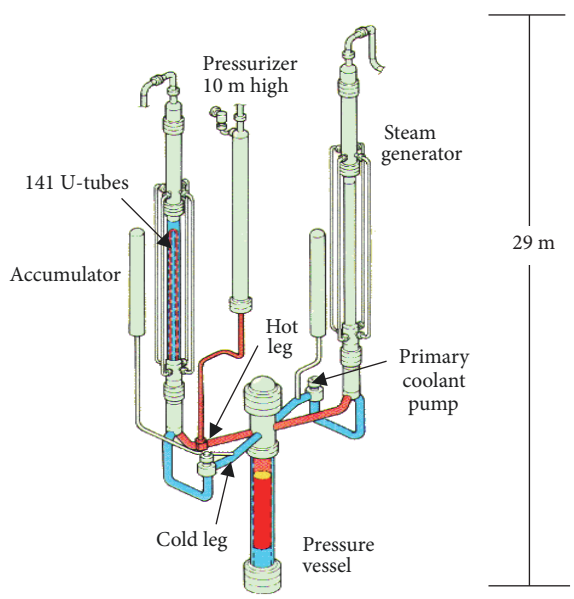

Figure 2: Schematic view of ROSA/LSTF [11].

the volumetric scale (2/48) and the ratio of the length to the square root of pipe diameter to better simulate the flow regime transitions in the primary loops (Froude number basis) [19]. The time scale of simulated thermal hydraulic phenomena is one to one to that in the reference PWR.

The LSTF core, 3.66 m in active height, consists of 1008 electrically heated rods in 24 rod bundles to simulate the fuel rod assembly in the reference PWR. This preserves the heat transfer characteristics of the core. The axial core power profile is a nine-step chopped cosine with a peaking factor of 1.495. The LSTF initial core power of 10 MW corresponds to 14% of the volumetric-scaled (1/48) PWR nominal core power because of a limitation in the capacity of power supply.

3. Common Conditions of Three LSTF Tests and RELAP5 Calculation Conditions

3.1. Common Conditions of Three LSTF Tests. The experiment was initiated by terminating feedwater in both SGs as well as by opening a break valve located downstream of the break orifice at time zero. At the same time, a scram signal was generated, causing the closure of main steam isolation valves in both SGs. The coastdown of primary coolant pumps was started at 18 s, and the pump rotation speed was decreased to zero 250 s after the initiation of the coastdown. Initial steady-state conditions such as PZR pressure and fluid temperatures in the hot and cold legs were 15.5 MPa, 598 K, and 562 K, respectively, according to the reference PWR conditions. The LSTF core power decay curve after the scram signal was predetermined on the basis of calculations with the RELAP5 code considering delayed neutron fission power and stored heat in PWR fuel rod [20] in addition to heat losses. The radial core power profile was assumed to be flat. The LSTF core power was maintained at the initial value of 10 MW for 18 s after the scram signal. The LSTF core power began to decay afterwards according to the specified core power. To obtain prototypical initial fluid temperature with this core

power, core flow rate was set to 14% of the scaled nominal flow rate. Initial SG secondary-side pressure was raised to 7.3 MPa to limit the primary-to-secondary heat transfer rate to 10 MW, while 6.1 MPa is nominal value in the reference PWR. Setpoint pressures for opening and closure of SG relief valves were 8.03 MPa and 7.82 MPa, respectively, referring to the corresponding values in the reference PWR.

Regarding the ECCS conditions, high-pressure injection system was totally failed. ACC system automatically initiated coolant injection into cold legs in both loops when the primary pressure decreases to 4.51 MPa according to the reference PWR. The ACC injection temperature of 320 K was the same as that in the reference PWR. As the AM measures, the SG secondary-side depressurization was done by fully opening the relief valves (inner diameter of 16.2 mm each) in both SGs, and the AFW was injected into the secondary-side of both SGs at the same time. The AFW flow rate was at a constant value of 0.7 kg/s for each SG until the SG secondary-side collapsed liquid level reached a certain high level and was controlled to keep the certain high level thereafter. This value of 0.7 kg/s corresponds to the volumetric-scaled rate of the reference PWR. The AFW temperature of 310 K was the same as that in the reference PWR. Coolant was injected from low-pressure injection system of ECCS into cold legs in both loops after the primary pressure decreases to a certain low pressure of below 1 MPa.

3.2. RELAP5 Calculation Conditions. For each of the three LSTF tests, the break was simulated with a sharp-edge orifice. The posttest analysis was conducted by employing the RELAP5/MOD3.3 code with a two-phase critical flow model, which has been proposed by Asaka et al. [21], to well predict the discharge rate through the sharp-edge orifice. The model employs the Bernoulli incompressible orifice flow equation with a discharge coefficient (C_d) of 0.61 for single-phase discharge liquid [22] and the maximum bounding flow theory for two-phase discharge flow [23]. This flow theory assumes that no phase change occurs at all along the flow and that the local slip ratio is equal to $(\rho_{liquid}/\rho_{gas})^{1/3}$, where ρ is the fluid density. A value of C_d of 0.84 was used for single-phase discharge steam [24]. Uncertainties should be included in the maximum bounding flow theory model for the prediction of two-phase break flow rate. To well predict the break flow rate, we adjusted C_d for two-phase discharge flow to 0.45, 0.55, and 0.61, respectively, for the analyses of TR-LF-18, TR-LF-17, and TR-LF-16 tests.

Figure 3 shows a noding schematic of LSTF for RELAP5 analysis. The LSTF system was modeled in one-dimensional manner including a pressure vessel, primary loops, PZR, SGs, and SG secondary-side system. The SG U-tubes were modeled by nine parallel flow channels that correspond to the nine different lengths of U-tubes, namely, 24 nodes for short-to-medium tubes (straight length of 9.44 m to 9.89 m, four cases in Table 1) and 26 nodes for medium-to-long tubes (straight length of 10.04 m to 10.64 m, five cases), for better prediction of the nonuniform flow behavior among the SG U-tubes under NC [25, 26], as observed in the three LSTF tests (to be mentioned in Sections 4.2, 5.2, and 6.2). The core was

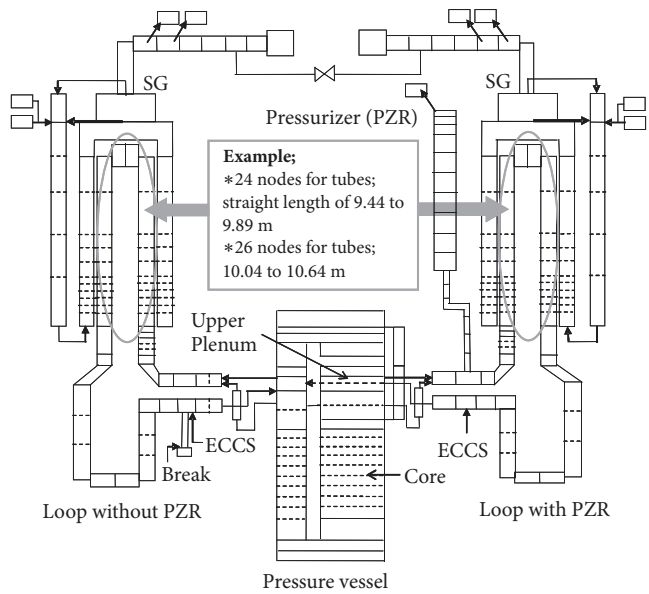

Figure 3: Noding schematic of LSTF for RELAP5 analysis [11].

represented by nine equal-height volumes that are vertically stacked according to nine-step chopped cosine power profile along the length of the core. The PZR was represented by ten vertical nodes to simulate the corresponding facility configuration. Other initial and boundary conditions were determined according to the LSTF test data.

In the RELAP5 code, the condensation heat transfer against influences of noncondensable gas is calculated by using the maximum value between the estimations based on the Shah model for turbulent flow [27] and on the Nusselt model for laminar flow [28] with the multipliers of the Vierow-Schrock correlation [29]. The multipliers concern the heat transfer degradation expressed as a function of gas mass fraction, which includes effects of the interfacial shear and the gas presence in a vertical tube at low pressures.

4. TR-LF-18 Test and RELAP5 Code Analysis

4.1. TR-LF-18 Test Conditions. The break was simulated by using a 7.2 mm inner diameter sharp-edge orifice, horizontally mounted at the downstream of a horizontal pipe that was connected to the cold leg wall. The orifice size corresponds to 0.5% of the volumetrically scaled cross-sectional area of the reference PWR cold leg. The SG secondary-side depressurization and the AFW injection into the SG secondary-side were initiated as the AM measures 10 min after the break.

4.2. Major Phenomena Observed in TR-LF-18 Test. Table 3 summarizes the chronology of major events in the TR-LF-18 test. Figures 4–11 show the major phenomena observed in the TR-LF-18 test. Break flow rate is derived from differential of time-integrated break flow evaluated from the liquid level increase in the break flow storage tank. The break flow rate roughly decreased stepwise when the break flow changed from single-phase liquid to two-phase flow at about 340 s

Table 3: Chronology of major events in LSTF tests.

Event	Time (s)		
	TR-LF-18	TR-LF-17	TR-LF-16
Break valve open, termination of feedwater in both SGs, and scram signal		0	
Start of primary coolant pumps coastdown		19	
Start of core power decay		21	
Stop of primary coolant pumps		269	
Empty PZR	145	370	410
Onset of SG secondary-side depressurization by fully opening relief valves in both SGs	602	1210	8
Onset of AFW injection into secondary-side of both SGs	615	1220	26
Initiation of ACC system in both loops	1200	1870	1470
Termination of ACC system in loop-A	2820	3810	6830
Termination of ACC system in loop-B	3040	4000	7320
Achievement of SG secondary-side liquid level up to 12 m	6000	7200	5600
Onset of primary depressurization by fully opening PZR relief valve	None	9400	12520
Primary pressure decrease to 1 MPa	7000	12900	15300
Start of coolant injection from low-pressure injection system into cold legs in both loops	8700	14400	17220
Break valve closure	9051	15063	18169
Core power off	9067	15090	18129

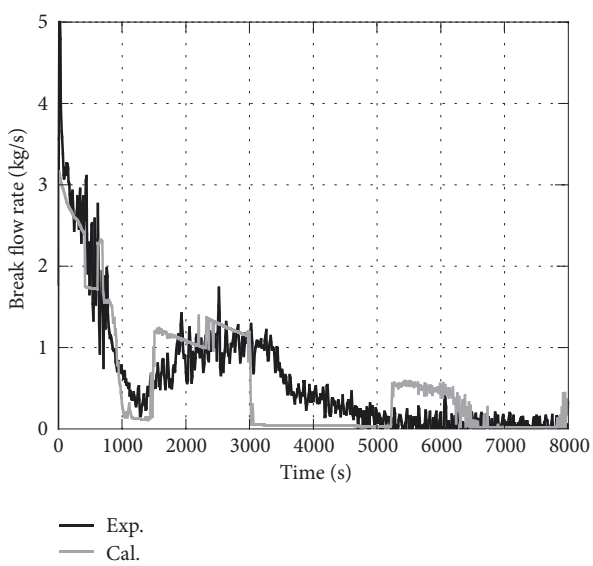

Figure 4: TR-LF-18 test and RELAP5 results for break flow rate.

first and then to single-phase vapor at around 6000 s (Figure 4). The primary pressure began to decrease after the break, whereas the SG secondary-side pressure increased to 8 MPa until the onset of the AM measures after the closure of the SG main steam isolation valves following the scram signal (Figure 5). The SG secondary-side pressure fluctuated between 8.03 MPa and 7.82 MPa due to cycle opening of the SG relief valves. The primary pressure decreased to the SG secondary-side pressure at around 450 s, implying that the AM measures may be ineffective to depressurize the primary system if the AM measures are initiated before around 450 s. The primary pressure followed the SG secondary-side pressure after the AM measures onset, which caused the actuation of ACC system (Figure 6). The SG secondary-side collapsed liquid level greatly decreased after the onset of the SG secondary-side depressurization and gradually recovered by the AFW injection into the SG secondary-side after around 2000 s (Figure 7).

The NC was established in both primary loops after the stop of the primary coolant pumps. The NC mass flow rate decreased almost to zero before the start of the ACC coolant injection (Figure 10), while coolant still remained in the SG U-tubes (Figures 8 and 9). Oscillation and no complete drain of coolant in the SG U-tubes may imply that two-phase NC may continue in some of U-tubes. The NC mass flow rate recovered following an increase in the primary mass inventory due to the ACC coolant injection (Figure 10). After the termination of the ACC coolant injection, the NC mass flow rate decreased somewhat differently in two loops depending probably on the different voiding conditions in the U-tubes between the two SGs. The collapsed liquid levels greatly decreased in most of the instrumented U-tubes after the nitrogen gas ingress, while two-phase NC continued with nitrogen gas through some of U-tubes (Figures 8 and 9). In the instrumented U-tubes (6 out of 141), different types of flow coexisted such as type of rapid coolant drain probably due to the nitrogen gas accumulation and type of continuous two-phase NC with nitrogen gas in one short tube (tube 1) of SG in loop A. Figure 11 shows the measured fluid temperatures near the top of instrumented U-tubes shown in Table 2 in loop A, taking account of the gas phase in the U-tubes after the completion of the ACC coolant injection (Figure 6).

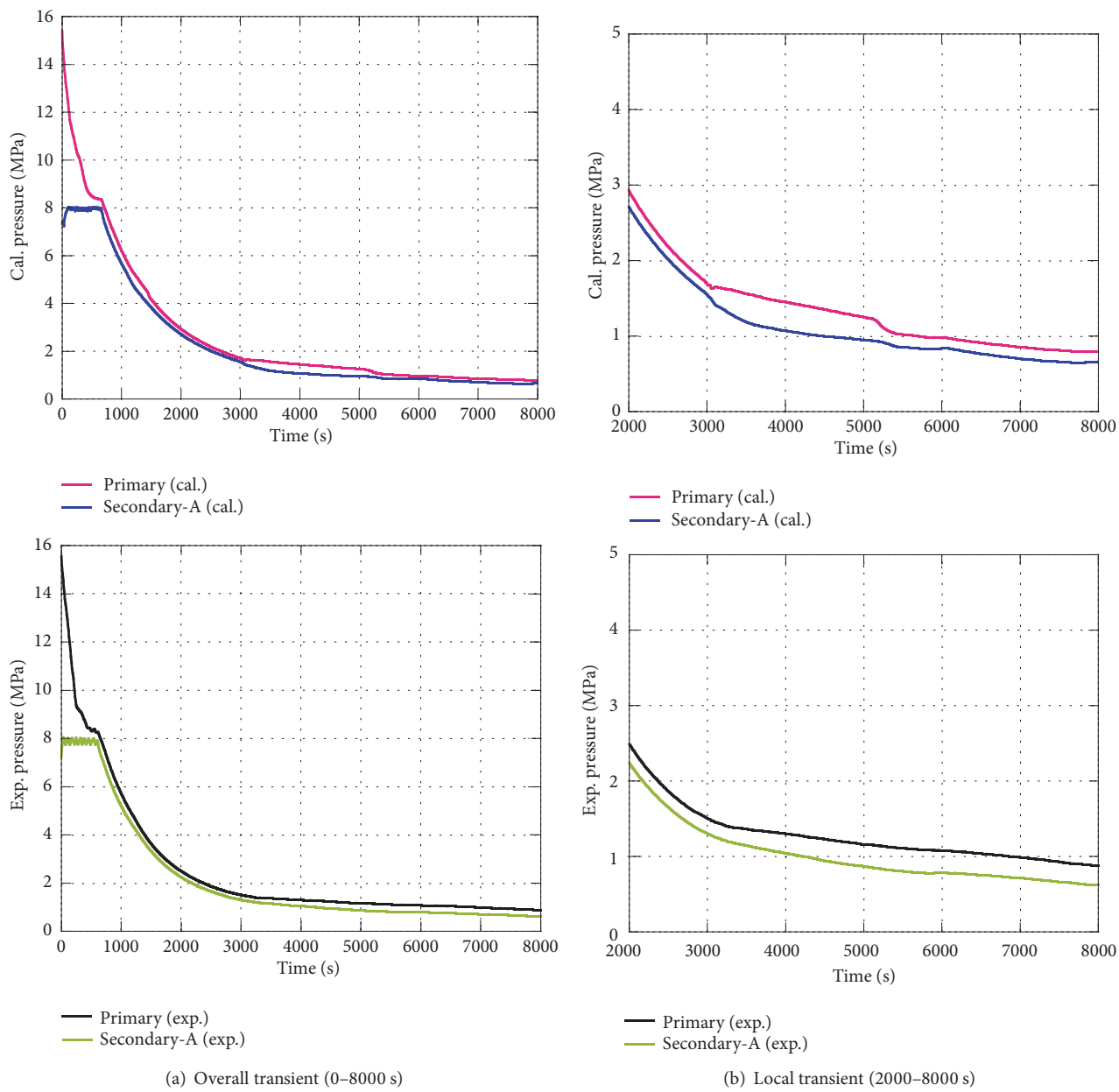

Figure 5: TR-LF-18 test and RELAP5 results for primary and SG secondary-side pressures in loop A.

The fluid temperatures were compared with the saturated temperature on the basis of the vessel upper plenum pressure as reference. The local gas phase temperatures near the top of the instrumented U-tubes other than one short tube (tube 1) became below the saturated temperature after around 3760 s, suggesting that nitrogen gas should accumulate in most of the SG U-tubes. The pressure difference became a little larger between the primary and the SG secondary sides because the nitrogen gas accumulated remarkably in the SG U-tubes after the termination of the ACC coolant injection (Figure 6). However, the primary pressure decreased to a certain low pressure of below 1 MPa probably due to the discharge of a part of nitrogen gas through the break. The NC and the AM measures contributed to maintain the core cooling effectively because of no core uncovery through the whole transient. The primary pressure was 0.87 MPa just before the coolant injection started from the low-pressure injection system into both the cold legs at 8700 s.

4.3. Comparison of Calculated Results with TR-LF-18 Test Data. The RELAP5/MOD3.3 code predicted mostly the overall trends of the major thermal hydraulic responses observed in the TR-LF-18 test. No core uncovery was reproduced through the whole transient. The code predicted the break flow rate reasonably well (Figure 4). In the calculated result, the reproduced primary depressurization worsened due to the nitrogen gas accumulation in the SG U-tubes (Figure 5). The SG secondary-side pressure was calculated reasonably

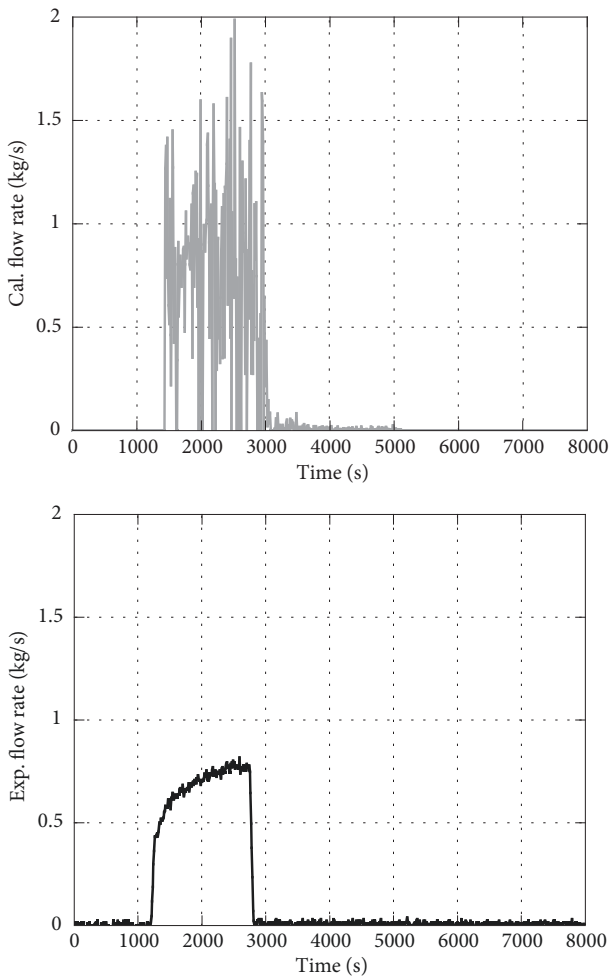

Figure 6: TR-LF-18 test and RELAP5 results for ACC flow rate in loop A.

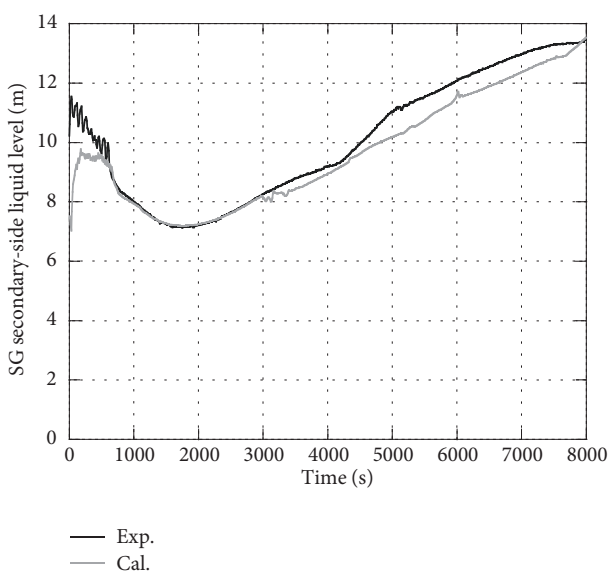

Figure 7: TR-LF-18 test and RELAP5 results for SG secondary-side collapsed liquid level in loop A.

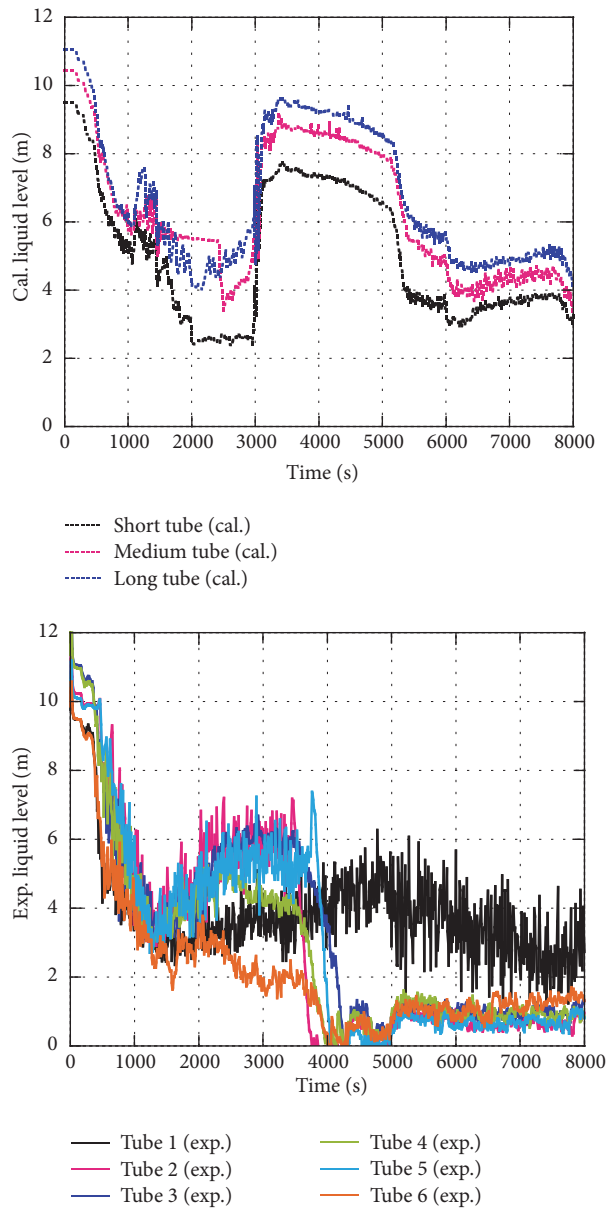

Figure 8: TR-LF-18 test and RELAP5 results for SG U-tube upflow-side collapsed liquid level in loop A.

well. The code, however, underpredicted the primary pressure after the nitrogen gas inflow, which may be caused by the overestimation in the condensation heat transfer in the SG U-tubes. The ACC flow rate was roughly predicted, though with significant fluctuation (Figure 6), due to influences of steam condensation in the cold leg volume where fluctuation occurred in the pressure. The ACC flow rate was larger in the calculation compared to the LSTF test, which caused larger fluctuation in the NC mass flow rate (Figure 10). The code underpredicted a little the SG secondary-side collapsed liquid level after around 3000 s (Figure 7). The code roughly calculated a tendency of coolant drain in some of U-tubes after the nitrogen gas ingress (Figures 8 and 9). In the calculation, however, the collapsed liquid levels monotonically

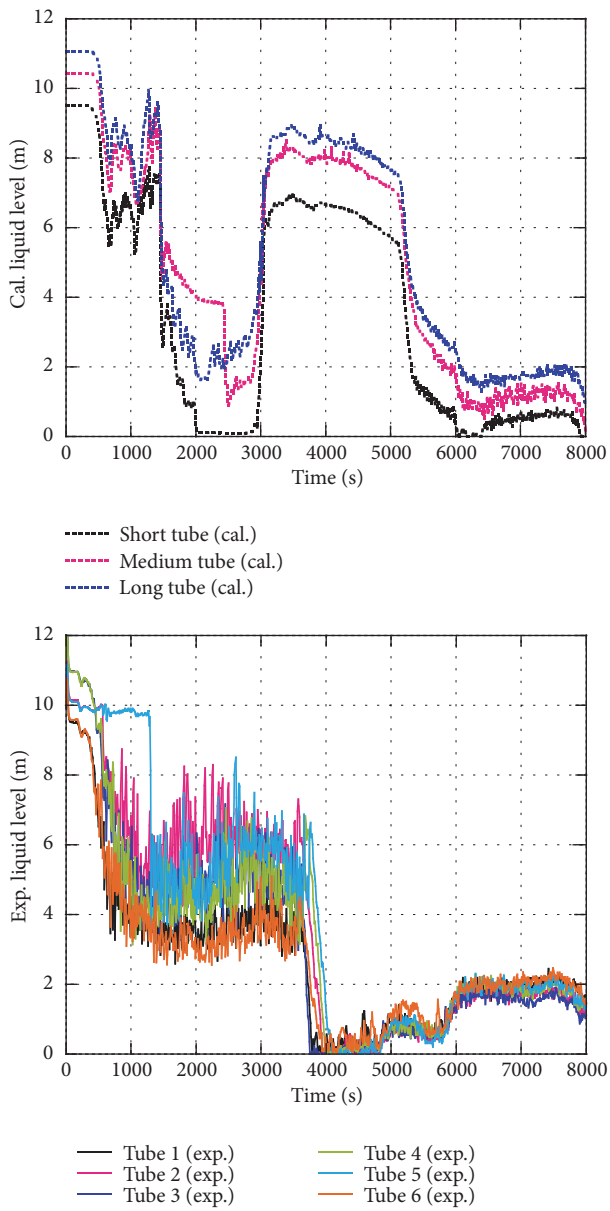

Figure 9: TR-LF-18 test and RELAP5 results for SG U-tube upflow-side collapsed liquid level in loop B.

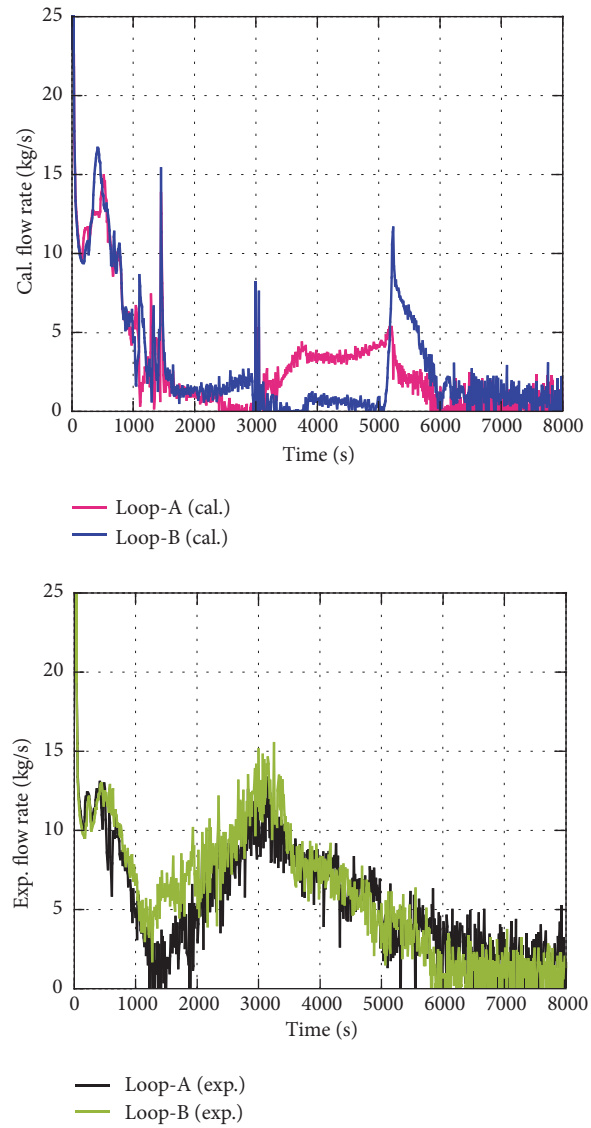

Figure 10: TR-LF-18 test and RELAP5 results for primary mass flow rate in each loop.

decreased with rather same drain rate among the U-tubes in both SGs. The trends of the collapsed liquid levels in the SG U-tubes in the calculation were similar to that in one short tube (tube 1) for loop A. The SG U-tube liquid levels almost became lost later in the calculation compared to the LSTF test for loop B. After the nitrogen gas inflow, the NC mass flow rate was not properly calculated (Figure 10) probably due to some discrepancies between the calculation and the LSTF test for the SG U-tube collapsed liquid levels.

The combination of the break size and the onset timing of the AM measures (i.e., the SG secondary-side depressurization and the AFW injection into the SG secondary-side) may affect the core collapsed liquid level, thus the cladding surface temperature. The occurrence probability of core uncovery and heatup should be higher as the break size is larger and the AM measures are initiated later. We performed sensitivity analysis based on the posttest analysis with the RELAP5 code in the case of the SBO transient with 0.5% cold leg break. The primary pressure decreased to the SG secondary-side pressure, while the SG secondary-side pressure fluctuated between 8.03 MPa and 7.82 MPa due to the cycle opening of the SG relief valves (Figure 12). Core temperature excursion would happen due to loss of the primary mass inventory through the break if no AM measures are taken until about 50 min after the break, while the primary pressure was kept constant at around 8 MPa (Figure 13). We assumed that the AM measures are initiated 60 min after the break following the start of core uncovery to investigate the influences of the AM measures on the core cooling. After the AM measures onset, the primary pressure decreased with a decrease in the SG secondary-side pressure, which caused the ACC system

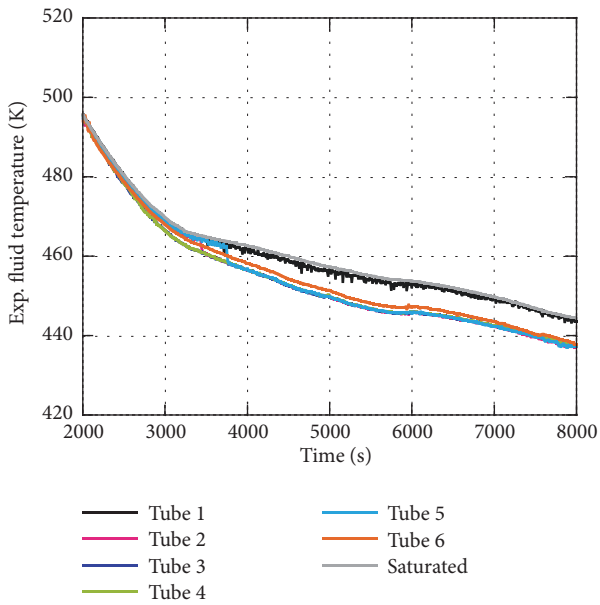

Figure 11: TR-LF-18 test results for fluid temperatures near top of SG U-tubes in loop A.

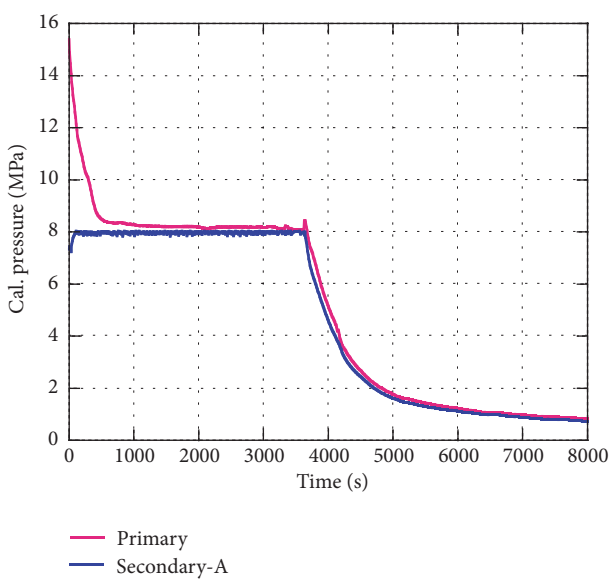

Figure 12: RELAP5 sensitivity analysis results for primary and SG secondary-side pressures in loop A.

actuation (Figure 12). Locations of the nodes of Positions 7 and 9, respectively, correspond to about 2.4–2.8 m and 3.2–3.6 m above the core bottom. The peak cladding temperature appeared at the node of Position 7, while the cladding surface temperature decreased later at the node of Position 9 than at the node of Position 7. The whole core was quenched because of an increase in the core collapsed liquid level due to the ACC coolant injection (Figure 13). The sensitivity analysis result by the RELAP5 code confirmed that the AM measures are effective for the core cooling.

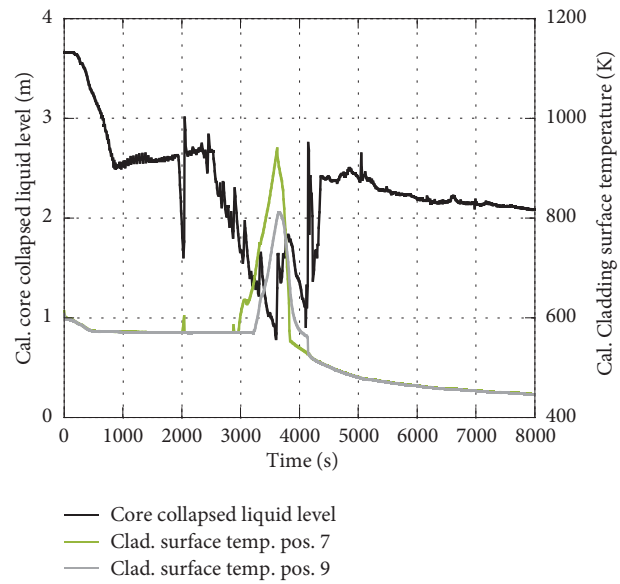

Figure 13: RELAP5 sensitivity analysis results for core collapsed liquid level and cladding surface temperature.

5. TR-LF-17 Test and RELAP5 Code Analysis

5.1. TR-LF-17 Test Conditions. The break was simulated by employing a 4.6 mm inner diameter sharp-edge orifice, horizontally mounted at the downstream of a horizontal pipe that was connected to the cold leg wall. The orifice size corresponds to 0.2% of the volumetrically scaled cross-sectional area of the reference PWR cold leg. The SG secondary-side depressurization and the AFW injection into the SG secondary-side were started as the AM measures 20 min after the break.

5.2. Major Phenomena Observed in TR-LF-17 Test. The chronology of major events in the TR-LF-17 test is summarized in Table 3. The major phenomena observed in the TR-LF-17 test are shown in Figures 14–22. The break flow turned from single-phase liquid to two-phase flow at about 660 s, which caused a decrease in the break flow rate, and then to single-phase vapor at around 9800 s (Figure 14). The primary pressure decreased to the SG secondary-side pressure at around 1000 s (Figure 15), which was later than in the TR-LF-18 test, implying that the AM measures may be ineffective for the primary depressurization if the AM measures are started before around 1000 s. During the time period around 40–530 s, the SG secondary-side pressure fluctuated between 8.7 MPa and 7.3 MPa due to unexpected failure of setting the pressures for the cycle opening of the SG relief valves, but there were no significant effects on the primary pressure. The primary pressure decreased following a decrease in the SG secondary-side pressure after the AM measures onset, which led to the ACC system actuation (Figure 16). A great decrease started in the SG secondary-side collapsed liquid level after the onset of the SG secondary-side depressurization, and a gradual level recovered in the SG secondary-side because of

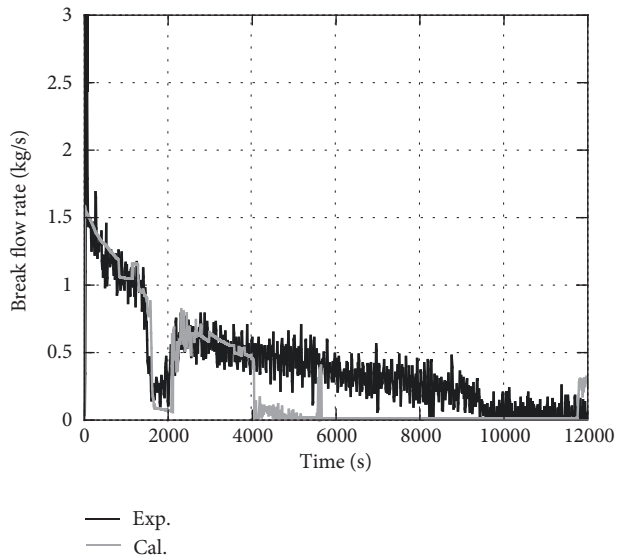

Figure 14: TR-LF-17 test and RELAP5 results for break flow rate.

the AFW injection into the SG secondary-side after around 2400 s (Figure 17).

The NC mass flow rate became close to zero before the ACC coolant injection initiation and recovered after an increase in the primary mass inventory by the ACC coolant injection (Figure 20). After the ACC coolant injection termination, the NC mass flow rate decreased differently in two loops depending probably on the drain conditions of coolant in the U-tubes between the two SGs rather than in the TR-LF-18 test. After the nitrogen gas ingress, the water column rapidly drained in the instrumented U-tubes of both SGs in nonuniform manner (Figures 18 and 19). The SG U-tubes became voided because of the nitrogen gas accumulation during the time period around 5300–8000 s in loop A and during the time period around 5300–7260 s in loop B. Figure 22 shows the measured fluid temperatures near the top of instrumented U-tubes in loop A, being compared with the saturated temperature. The degree of subcooling near the top of two short tubes (tubes 1 and 6) was smaller than that near the top of other tubes by around 5200 s. This suggests that two-phase NC with nitrogen gas should continue in the two short tubes. Large pressure difference appeared between the primary and SG secondary sides because the remarkable nitrogen gas accumulation occurred in the SG U-tubes after the ACC coolant injection completion (Figure 15). The primary depressurization rate was smaller than in the TR-LF-18 test probably because the amount of the nitrogen gas discharged through the break was small. An optional AM measure was initiated by fully opening the PZR relief valve (inner diameter of 10.18 mm) at 9400 s to enhance the primary depressurization, which caused that the primary pressure decreased to a certain low pressure of below 1 MPa (Figure 15) and an increase occurred in the PZR liquid level (Figure 21). The NC and the AM measures were confirmed to be effective for the core cooling because of no core uncovery through the whole transient. The primary pressure was 0.94 MPa just before the coolant was injected from the low-pressure injection system into both the cold legs at 14400 s.

5.3. Comparison of Calculated Results with TR-LF-17 Test Data. Most of the overall trends of the major thermal hydraulic responses observed in the TR-LF-17 test were predicted by the RELAP5/MOD3.3 code. The calculated result reproduced no core uncovery through the whole transient. The break flow rate was predicted reasonably well (Figure 14). In the calculated result, the reproduced primary depressurization rate decreased due to the nitrogen gas accumulation in the SG U-tubes (Figure 15). Only in the calculation, we unchanged the setpoint pressures for the cycle opening of the SG relief valves. The SG secondary-side pressure was properly calculated after the SG secondary-side depressurization onset. The primary pressure, however, was underpredicted after the nitrogen gas inflow probably due to the overestimation in the condensation heat transfer in the SG U-tubes. The primary depressurization by fully opening the PZR relief valve as the optional AM measure was started at 9000 s in the calculation, whereas it was initiated at 9400 s in the LSTF test. After the optional AM measure onset, the PZR liquid level was roughly calculated, though with large fluctuation (Figure 21). The code roughly calculated the ACC flow rate, though with significant fluctuation (Figure 16). The ACC flow rate in the calculation was larger than that in the LSTF test, which led to larger fluctuation in the NC mass flow rate (Figure 20). The SG secondary-side collapsed liquid level was a little overpredicted during the time period around 1300–4000 s, while it was slightly underpredicted during the time period around 5600–8000 s (Figure 17). The code roughly predicted the trends of the collapsed liquid levels in the SG U-tubes (Figures 18 and 19). The code calculation, however, showed that the collapsed liquid levels monotonically dropped with rather same drain rate among the U-tubes in both SGs. The SG U-tubes became empty of liquid later in the calculation compared to the LSTF test. After the nitrogen gas ingress, the code did not properly calculate the NC mass flow rate (Figure 20) probably due to some differences between the calculation and the LSTF test for the SG U-tube collapsed liquid levels.

When PWR accidents are analyzed using best-estimate computer codes, simplified input models are usually employed such that many U-tubes in each SG are lumped into one equivalent tube in view of reducing the calculation time [30]. However, the simplified input models are inapplicable to the PWR accidents where nonuniform flow happens among the U-tubes under NC. In the posttest analyses for the TR-LF-18 and TR-LF-17 tests, the trend of coolant drain was roughly calculated in some of U-tubes after the nitrogen gas inflow (shown in Figures 8, 9, 18, and 19) by modeling the SG U-tubes with nine parallel flow channels in which nine tubes with different lengths were simulated by 24 or 26 nodes. A detailed modeling of the SG U-tubes with fine-mesh multiple parallel flow channels would thus be necessary when such complex NC phenomena with nitrogen gas are included in the PWR accidents.

6. TR-LF-16 Test and RELAP5 Code Analysis

6.1. TR-LF-16 Test Conditions. The break was simulated by using a 3.4 mm inner diameter sharp-edge orifice, upwardly

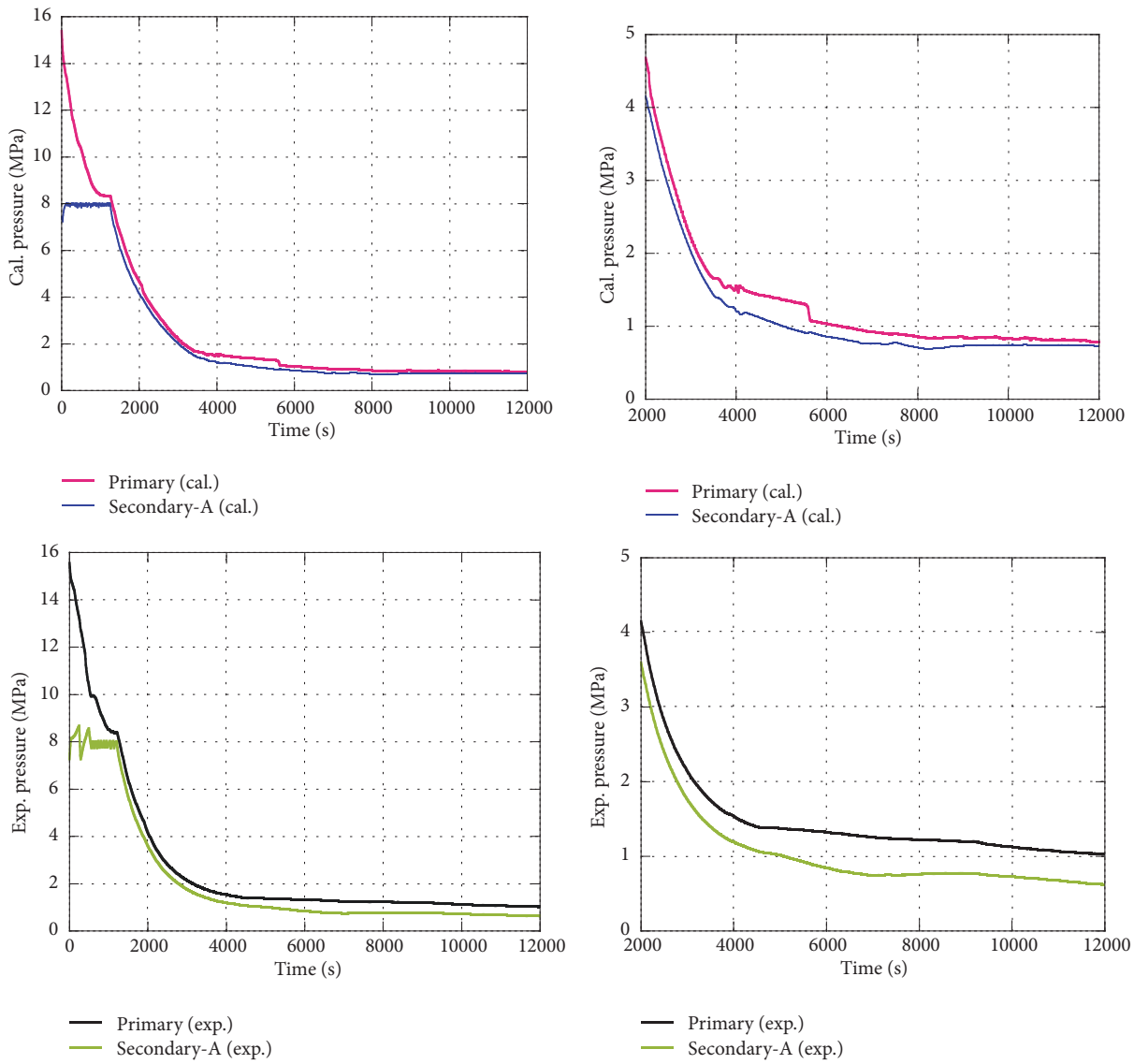

(a) Overall transient (0–12000 s)

(b) Local transient (2000–12000 s)

Figure 15: TR-LF-17 test and RELAP5 results for primary and SG secondary-side pressures in loop A.

mounted at the downstream of a horizontal pipe that was connected to the cold leg wall. The orifice size corresponds to 0.1% of the volumetrically scaled cross-sectional area of the reference PWR cold leg. The AM measures (i.e., the SG secondary-side depressurization and the AFW injection into the SG secondary-side) were initiated simultaneously with the break.

6.2. Major Phenomena Observed in TR-LF-16 Test. Table 3 summarizes the chronology of major events in the TR-LF-16 test. Figures 23–30 show the major phenomena observed in the TR-LF-16 test. The break flow became in two-phase flow after about 1150 s, which led to a decrease in the break flow rate (Figure 23). Extremely small size of break caused a slow primary depressurization (Figure 24). By contrast, a great decrease started in the SG secondary-side pressure concurrently with the break. The primary pressure thus was higher than the SG secondary-side pressure through the whole transient. The ACC system actuated later than in the TR-LF-18 test (Figure 25), whereas the AM measures were started much earlier than in the TR-LF-18 test. In the case of the SBO transient with 0.1% cold leg break, the effective AM measures may be possible to depressurize the primary system if the AM measures are initiated after around 2000 s, referring to the result of the previous LSTF test [15] on the PWR SBO transient with the pump seal leakage (simulated by 0.1% cold leg break). The SG secondary-side collapsed liquid level began to decrease simultaneously with the break and gradually recovered through the AFW injection into the SG secondary-side after around 2000 s (Figure 26).

The NC mass flow rate recovered with an increase in the primary mass inventory because of the ACC coolant injection

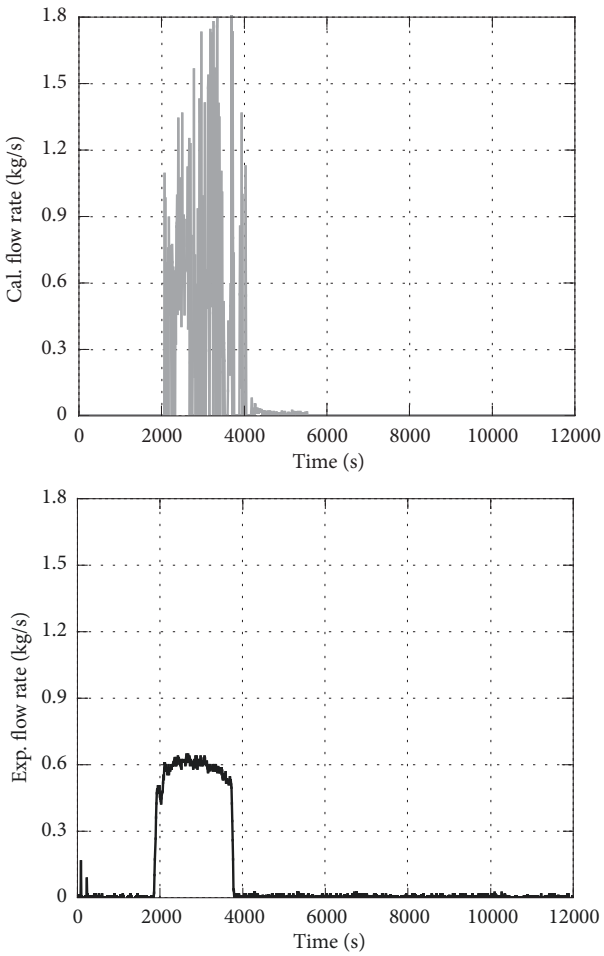

Figure 16: TR-LF-17 test and RELAP5 results for ACC flow rate in loop A.

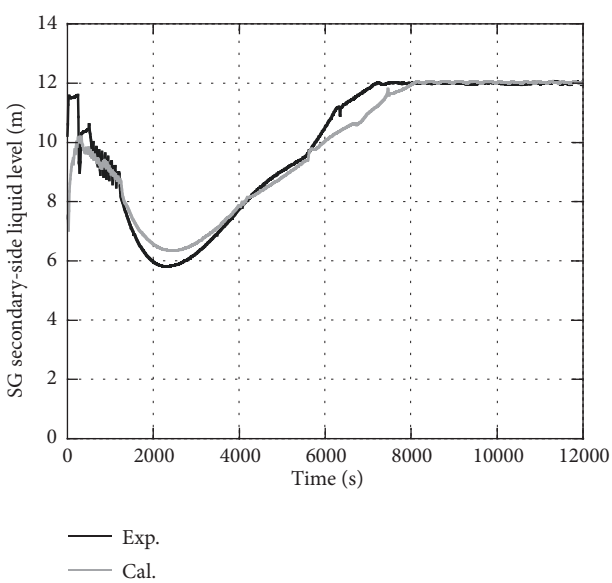

Figure 17: TR-LF-17 test and RELAP5 results for SG secondary-side collapsed liquid level in loop A.

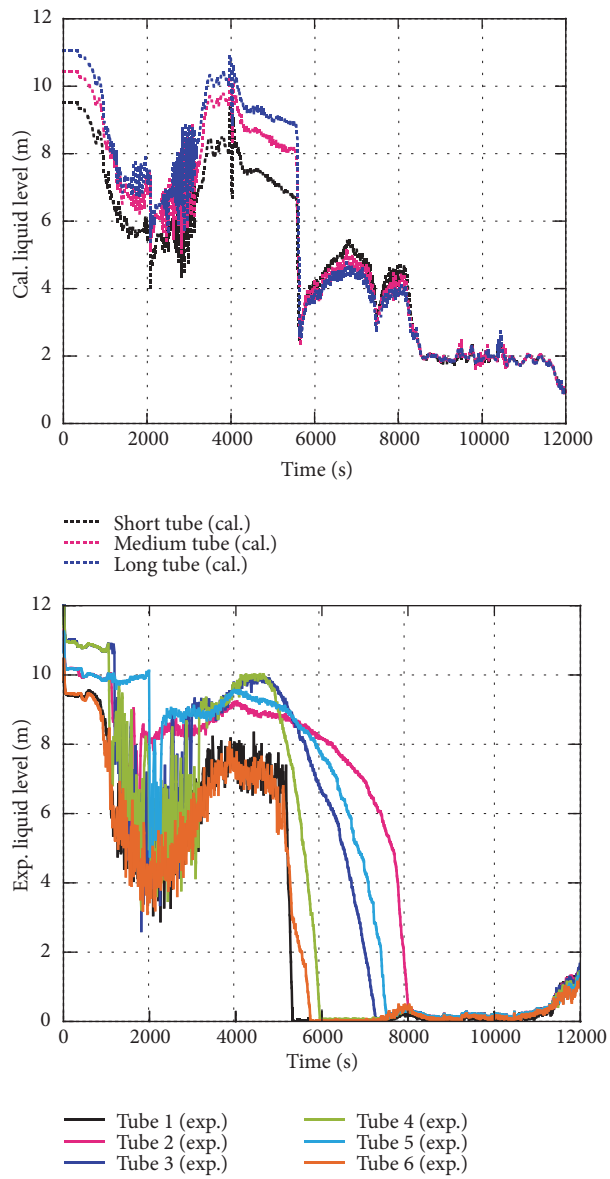

Figure 18: TR-LF-17 test and RELAP5 results for SG U-tube upflow-side collapsed liquid level in loop A.

and remained constant at a certain low flow rate after the ACC coolant injection termination (Figure 29). The U-tubes of both SGs were mostly filled with water even after the ACC coolant injection completion due to the extremely small-break size (Figures 27 and 28). An optional AM measure was initiated by fully opening the PZR relief valve (10.18 mm in inner diameter) at 12520 s for the enhanced primary depressurization because the primary pressure decreased much slower than in the TR-LF-18 test. The optional AM measure caused the primary pressure to decrease to a certain low pressure of below 1 MPa (Figure 24) and an increase occurred in the PZR liquid level (Figure 30). Most of nitrogen gas was discharged through the PZR relief valve and the break because of the almost full SG U-tubes at the ACC coolant injection termination, and thus there were no effects

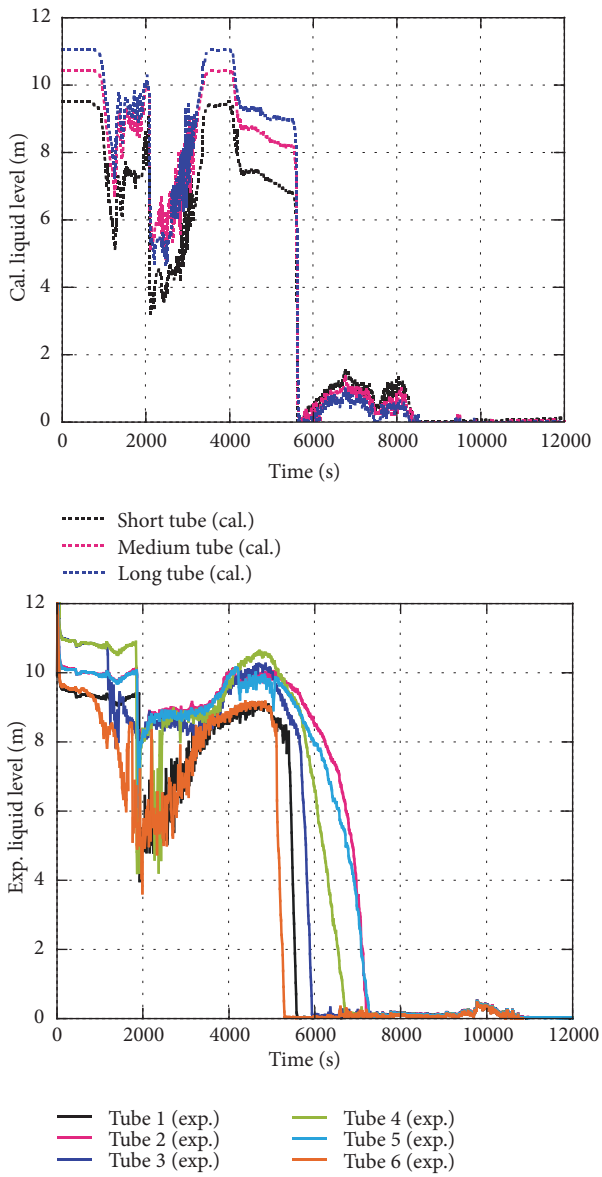

Figure 19: TR-LF-17 test and RELAP5 results for SG U-tube upflow-side collapsed liquid level in loop B.

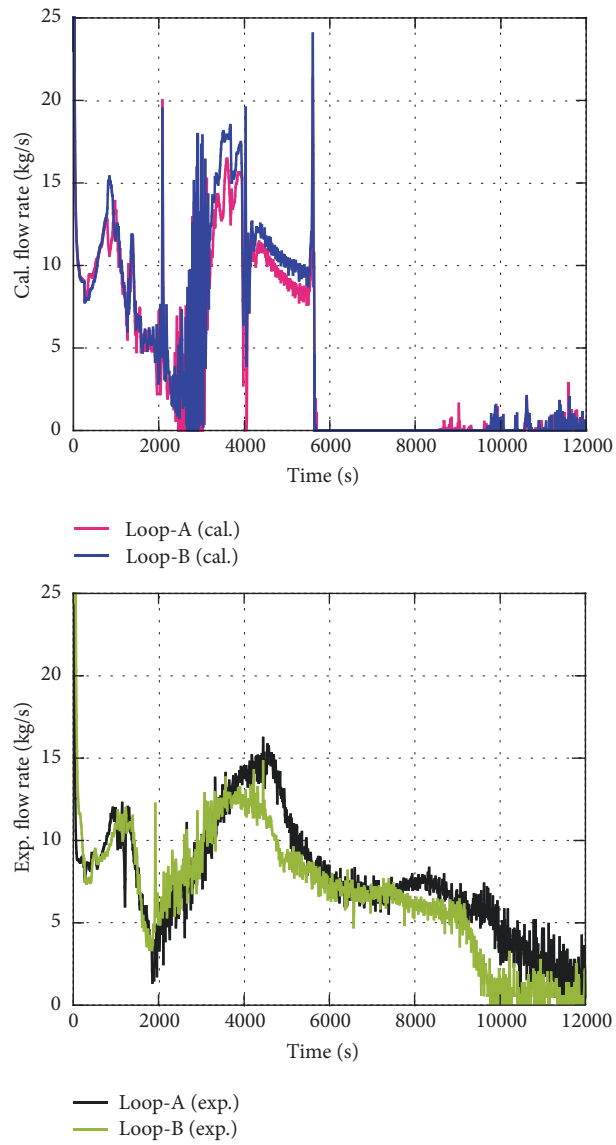

Figure 20: TR-LF-17 test and RELAP5 results for primary mass flow rate in each loop.

of nitrogen gas on the primary depressurization. After the optional AM measure onset, a great level drop started in the instrumented U-tubes of both SGs in nonuniform manner (Figures 27 and 28), which caused asymmetric NC between two loops (Figure 29). The drain rates of coolant in the instrumented U-tubes in loop B were larger than those in loop A due to the break effect. The drain rate of coolant in one short tube (tube 6) was the largest and that in one medium tube (tube 2) was the smallest for loop A. One medium tube (tube 2) became empty of liquid, the latest for loop B. The NC played an important role in the core cooling because of no core uncovery through the whole transient. The primary pressure was 0.92 MPa just before the coolant injection started from the low-pressure injection system into both the cold legs at 17220 s.

6.3. Comparison of Calculated Results with TR-LF-16 Test Data. The RELAP5/MOD3.3 code predicted mostly the overall trends of the major thermal hydraulic responses observed in the TR-LF-16 test. No core uncovery was reproduced through the whole transient. The primary pressure was a little overpredicted probably due to some discrepancies between the calculation and the LSTF test for the break flow rate and the ACC flow rate (Figures 23–25). By contrast, the SG secondary-side pressure was calculated reasonably well (Figure 24). The primary depressurization by fully opening the PZR relief valve as the optional AM measure was started at 11000 s in the calculation, whereas it was initiated at 12520 s in the LSTF test. After the optional AM measure onset, the primary pressure decreased to the SG secondary-side pressure earlier in the calculation compared to the LSTF test (Figure 24). After the optional AM measure onset, the PZR

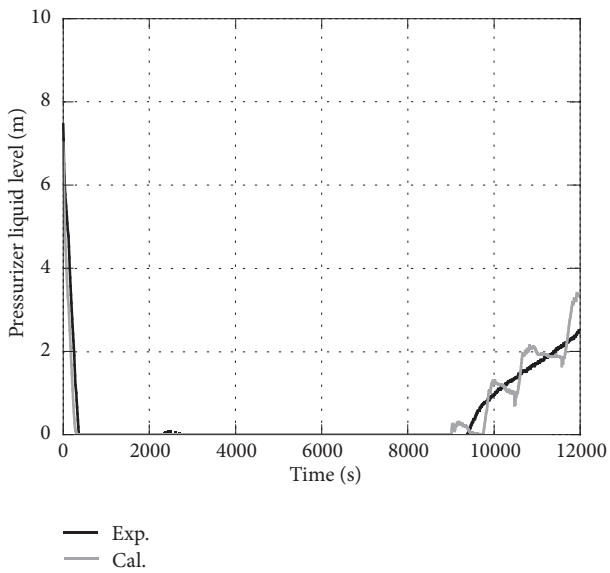

Figure 21: TR-LF-17 test and RELAP5 results for PZR liquid level.

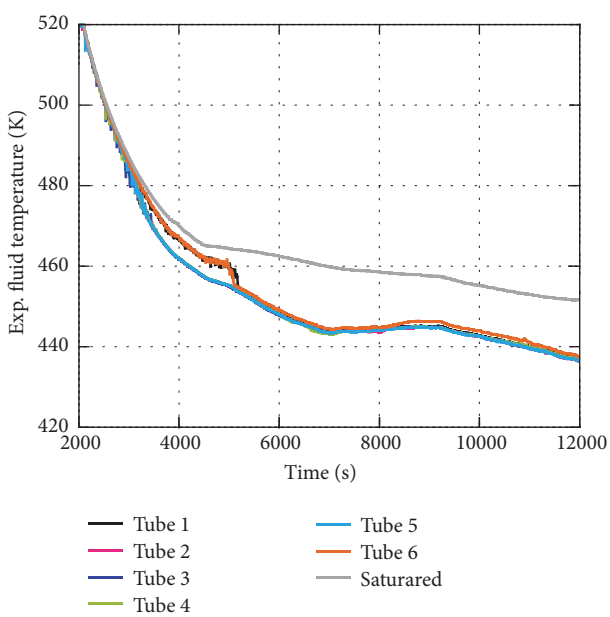

Figure 22: TR-LF-17 test results for fluid temperatures near top of SG U-tubes in loop A.

liquid level was roughly predicted, though with large fluctuation (Figure 30). The code calculation showed that the ACC flow rate was larger with significant fluctuation compared to the LSTF test (Figure 25). The SG secondary-side collapsed liquid level was predicted reasonably well (Figure 26). After the optional AM measure onset, in the calculated result, the reproduced collapsed liquid levels greatly dropped in most of the SG U-tubes (Figures 27 and 28). In the calculation, however, the collapsed liquid levels monotonically decreased with rather same drain rate among the U-tubes in both SGs. The trends of the collapsed liquid levels in the SG U-tubes were similar to that in one short tube (tube 6) for loop A,

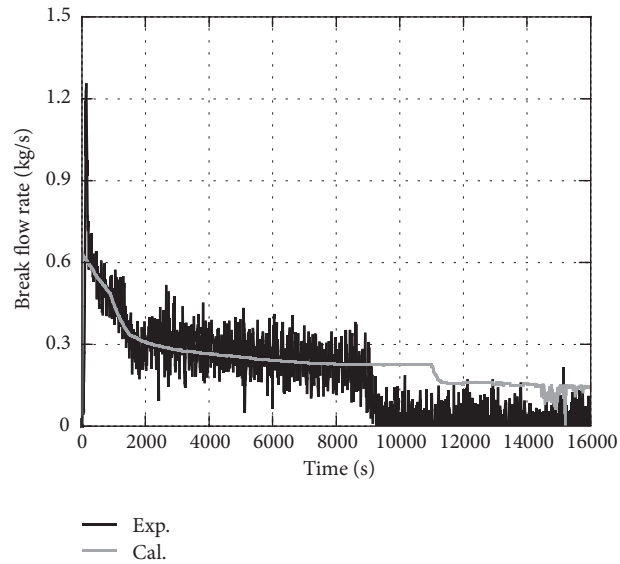

Figure 23: TR-LF-16 test and RELAP5 results for break flow rate.

while they were similar to that in one medium tube (tube 2) for loop B. After the optional AM measure onset, the code failed to calculate the asymmetric NC mass flow rate between two loops with no significant increase (Figure 29) probably due to some differences between the calculation and the LSTF test for the SG U-tube collapsed liquid levels.

7. Conclusions

Three ROSA/LSTF tests were carried out simulating AM measures during PWR SBO transient with loss of primary coolant under assumptions of nitrogen gas ingress and totally failed high-pressure injection system. The AM measures were SG secondary-side depressurization by fully opening the relief valves in both SGs and AFW injection into the secondary-side of both SGs simultaneously. The results of the three LSTF tests were compared mutually to make clear the influences of the break size and the onset timing of the AM measures. The results of the three LSTF tests were compared with the posttest analysis results by the RELAP5/MOD3.3 code to clarify the remaining subjects. Major results are summarized as follows:

(1) In the three LSTF tests, the primary pressure decreased to a certain low pressure of below 1 MPa with or without the primary depressurization by fully opening the PZR relief valve as the optional AM measure, while no core uncovery took place through the whole transient. Nonuniform flow occurred among the SG U-tubes under NC with nitrogen gas depending probably on the gas accumulation rate in the TR-LF-18 and TR-LF-17 tests that the gas accumulated remarkably. The primary depressurization rate was smaller in the TR-LF-17 test than in the TR-LF-18 test probably because the amount of the nitrogen gas discharged through the break was small. In the TR-LF-16 test, most of nitrogen gas was discharged through

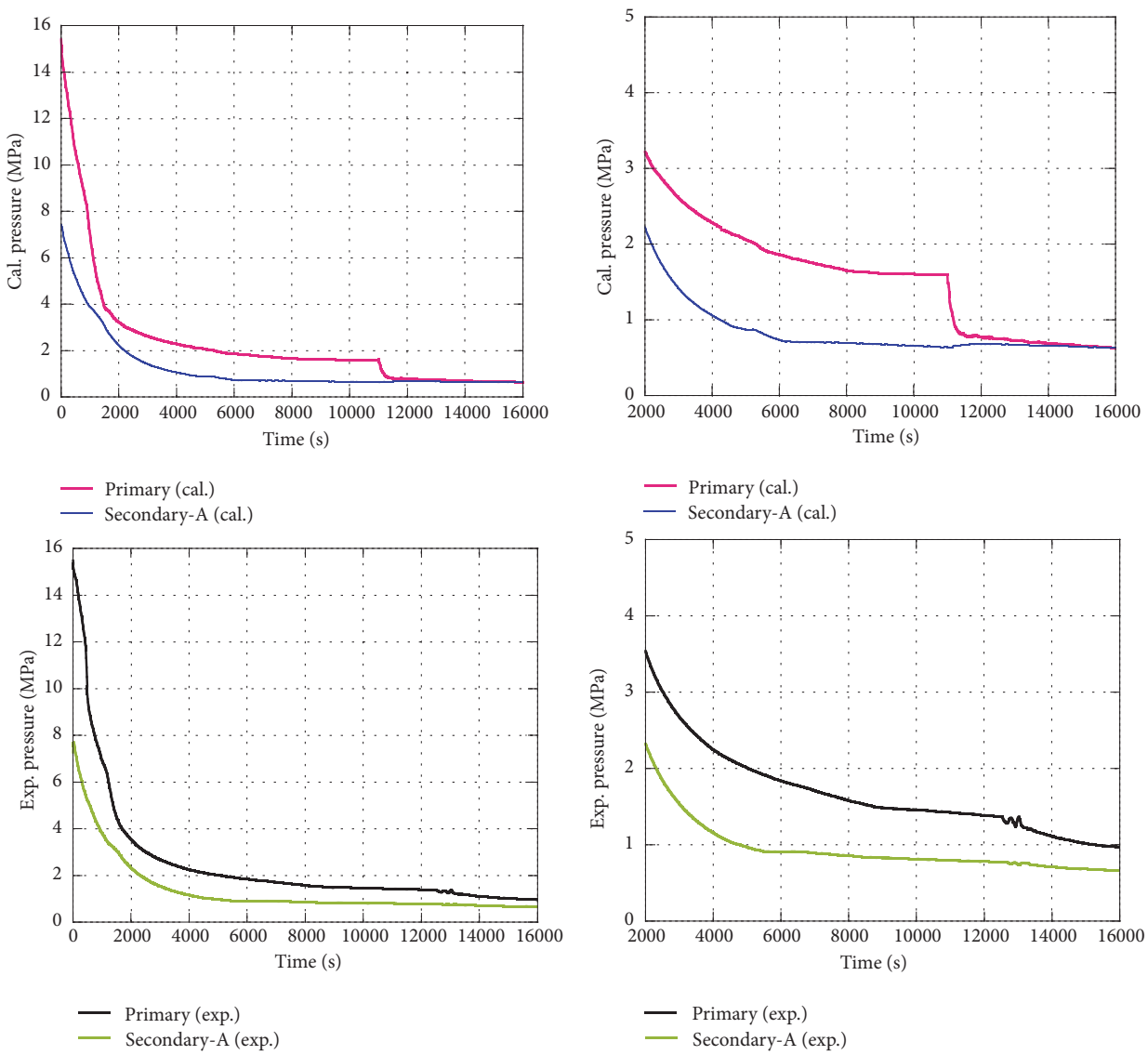

(a) Overall transient (0–16000 s)

(b) Local transient (2000–16000 s)

Figure 24: TR-LF-16 test and RELAP5 results for primary and SG secondary-side pressures in loop A.

the PZR relief valve and the break because of the almost full SG U-tubes at the ACC coolant injection completion due to the extremely small size of break, which resulted in no effects of nitrogen gas on the primary depressurization.

(2) The RELAP5/MOD3.3 code predicted most of the overall trends of the major thermal hydraulic responses observed in the three LSTF tests. Some discrepancies from the measured data, however, appeared in the SG U-tube collapsed liquid levels and the NC mass flow rate after the nitrogen gas inflow as well as the ACC flow rate through the analyses for the TR-LF-18 and TR-LF-17 tests that the remarkable gas accumulation occurred. The code also underpredicted the primary pressure after the nitrogen gas ingress, which may be caused by the overestimation in the condensation heat transfer in the SG U-tubes.

The obtained experimental database on the SBO with loss of primary coolant will be helpful in considering appropriate safety assurance measures in PWR accident scenarios taking severe multiple system failures into account and in improving the understanding of the degradation in the primary depressurization due to nitrogen gas ingress under NC when the primary pressure decreases to below 1 MPa. An insight was obtained from the posttest analyses by the RELAP5 code that detailed modeling of SG U-tubes with fine-mesh multiple parallel flow channels would be needed in case of PWR accidents where nonuniform flow happens among the U-tubes under NC.

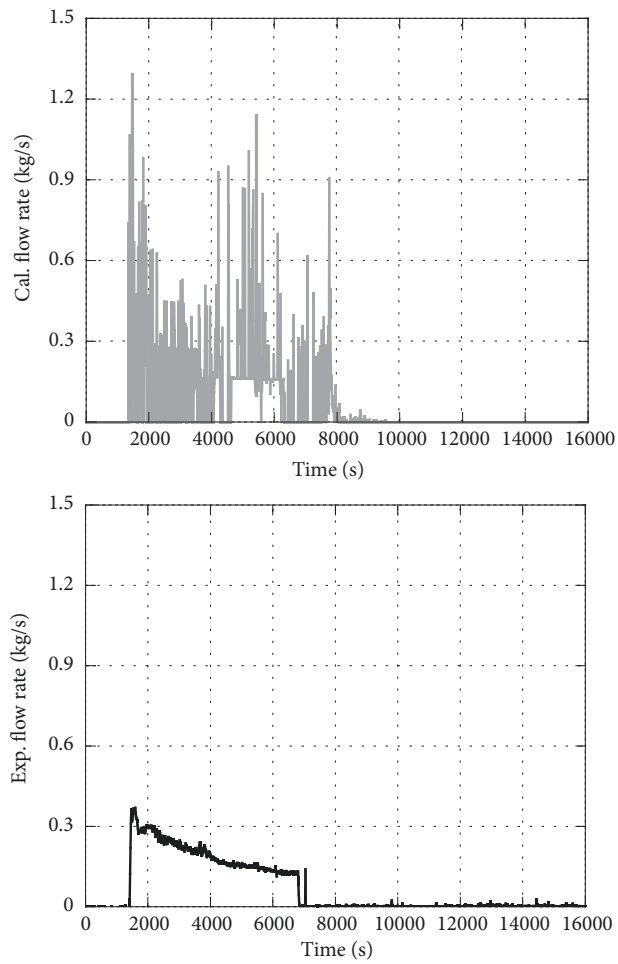

Figure 25: TR-LF-16 test and RELAP5 results for ACC flow rate in loop A.

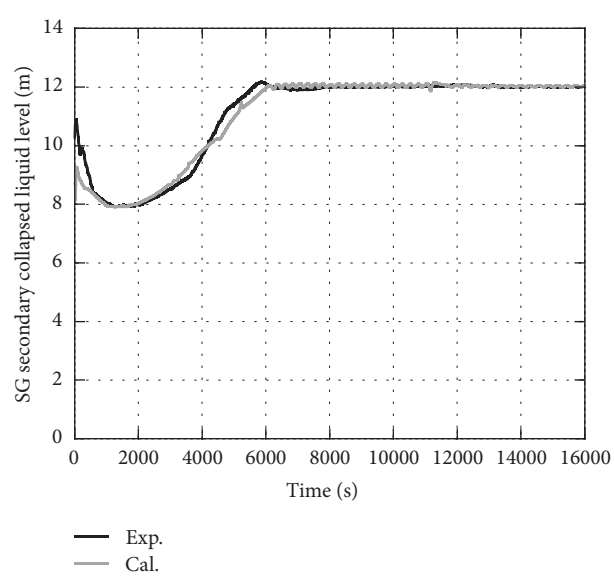

Figure 26: TR-LF-16 test and RELAP5 results for SG secondary-side collapsed liquid level in loop A.

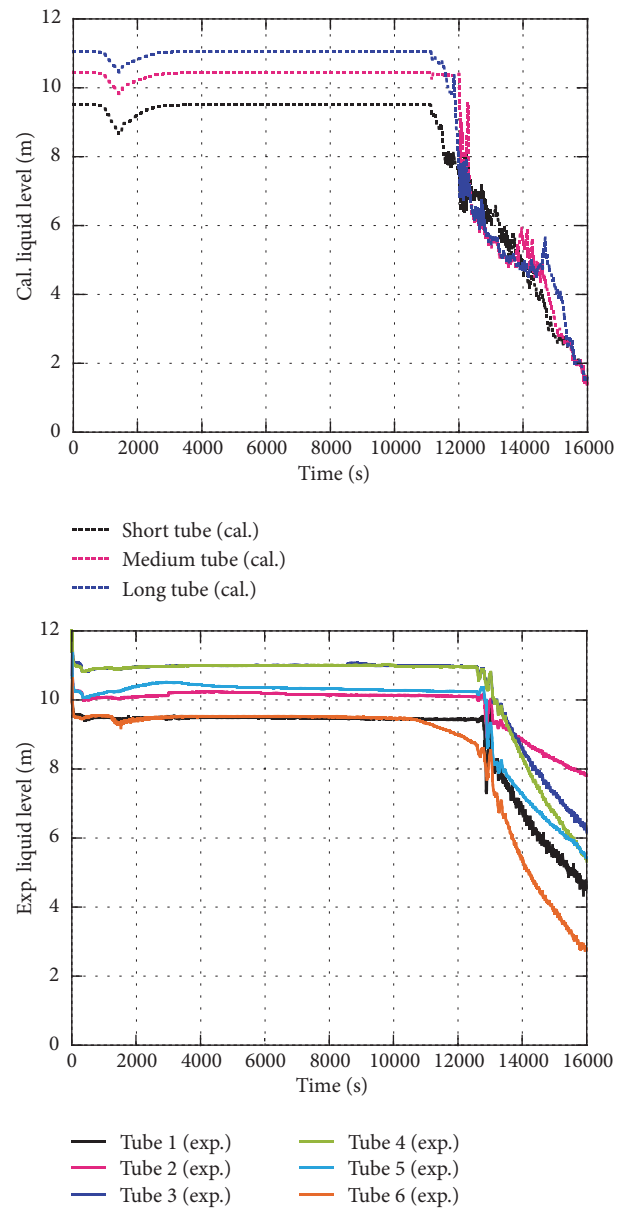

Figure 27: TR-LF-16 test and RELAP5 results for SG U-tube upflow-side collapsed liquid level in loop A.

Nomenclature

ACC: Accumulator
AFW: Auxiliary feedwater
AM: Accident management
C_d: Discharge coefficient
ECCS: Emergency core cooling system
LSTF: Large-scale test facility
NC: Natural circulation
PKL: Primärkreisläufe versuchsanlage
PSB: Polnomasshtabnyi stend besopasnosti
PWR: Pressurized water reactor
PZR: Pressurizer
ROSA: Rig of safety assessment

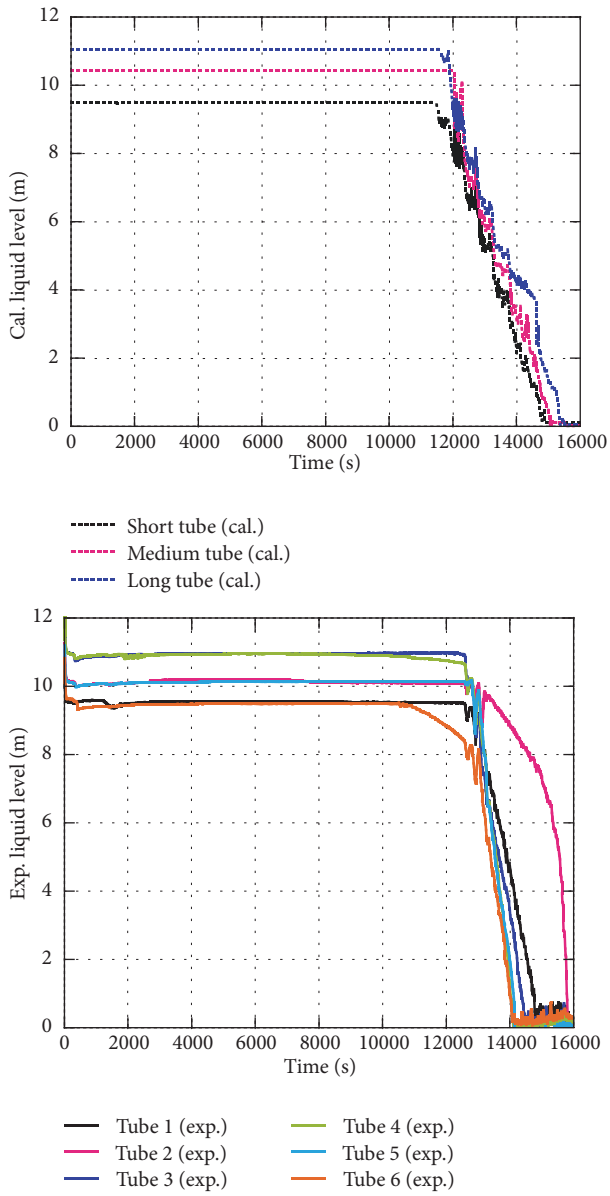

Figure 28: TR-LF-16 test and RELAP5 results for SG U-tube upflow-side collapsed liquid level in loop B.

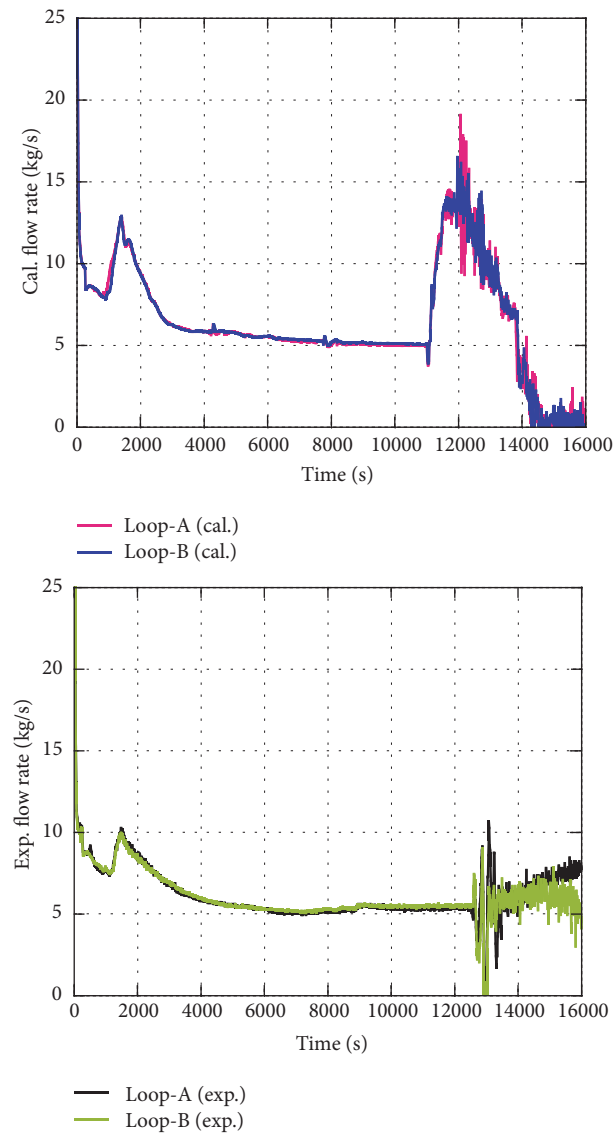

Figure 29: TR-LF-16 test and RELAP5 results for primary mass flow rate in each loop.

SBO: Station blackout
SG: Steam generator
VVER: Vodo-vodianoi energeticheskii reaktor.

Data Availability

The LSTF (large-scale test facility) tests were conducted under the auspices of Nuclear Regulation Authority, Japan (NRA). Therefore, the experimental data, shown in Figures 4–30 as well as Table 3 of the manuscript, used to support the findings of this study have not been made available because of the restriction by the NRA. Other data, including calculated results by RELAP5/MOD3.3 code, used to support the findings of this study are available from the corresponding author (Takeshi Takeda) upon request.

Disclosure

An earlier version of this work was presented at "the Japan Atomic Energy Society Annual Meeting in the Spring of 2017."

Conflicts of Interest

The authors declare that there are no conflicts of interest regarding the publication of this paper.

Acknowledgments

The LSTF tests were conducted under the auspices of Nuclear Regulation Authority, Japan. The authors would like to thank Messrs. M. Ogawa and A. Ohwada of Japan Atomic Energy Agency for performing the LSTF tests under collaboration with members from Nuclear Engineering Co. as well as Miss

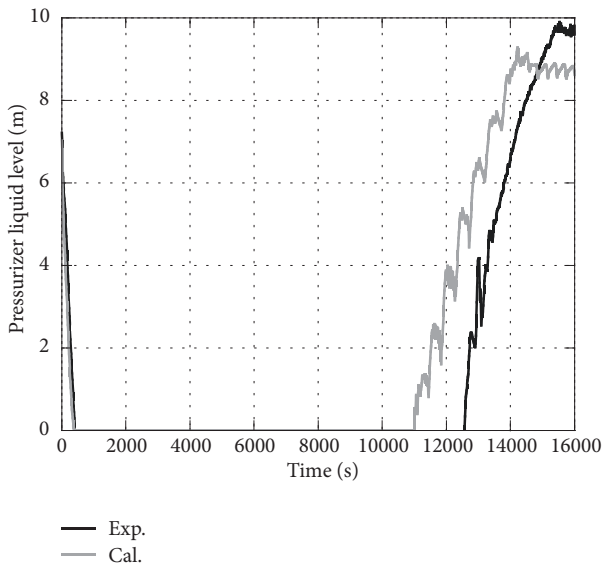

Figure 30: TR-LF-16 test and RELAP5 results for PZR liquid level.

K. Toyoda of Research Organization for Information Science and Technology for manipulating the data of the LSTF tests.

References

[1] M. Hirano, T. Yonomoto, M. Ishigaki et al., "Insights from review and analysis of the Fukushima Dai-ichi accident," *Journal of Nuclear Science and Technology*, vol. 49, no. 1, pp. 1–17, 2012.

[2] M. Cherubini, N. Muellner, F. D'auria, and G. Petrangeli, "Application of an optimized AM procedure following a SBO in a VVER-1000," *Nuclear Engineering and Design*, vol. 238, no. 1, pp. 74–80, 2008.

[3] A. Prošek and L. Cizelj, "Long-term station blackout accident analyses of a PWR with RELAP5/MOD3.3," *Science and Technology of Nuclear Installations*, vol. 2013, Article ID 851987, 15 pages, 2013.

[4] P. Tusheva, F. Schäfer, N. Reinke et al., "Assessment of accident management measures on early in-vessel station blackout sequence at VVER-1000 pressurized water reactors," *Nuclear Engineering and Design*, vol. 277, pp. 106–116, 2014.

[5] R. V. Gencheva, A. E. Stefanova, and P. P. Groudev, "Investigation of station blackout scenario in VVER440/v230 with RELAP5 computer code," *Nuclear Engineering and Design*, vol. 295, pp. 441–456, 2015.

[6] H.-T. Lin, J.-R. Wang, K.-C. Huang, C. Shih, S.-C. Chiang, and C.-C. Liu, "Station blackout mitigation strategies analysis for Maanshan PWR plant using TRACE," *Annals of Nuclear Energy*, vol. 89, pp. 1–18, 2016.

[7] B. Chatterjee, D. Mukhopadhyay, H. G. Lele et al., "Analyses for VVER-1000/320 reactor for spectrum of break sizes along with SBO," *Annals of Nuclear Energy*, vol. 37, no. 3, pp. 359–370, 2010.

[8] S. Šadek, D. Grgić, and Z. Šimić, "Application of ASTEC, MELCOR, and MAAP Computer Codes for Thermal Hydraulic Analysis of a PWR Containment Equipped with the PCFV and PAR Systems," *Science and Technology of Nuclear Installations*, vol. 2017, Article ID 8431934, 16 pages, 2017.

[9] A. Bucalossi, A. Del Nevo, F. Moretti, F. D'Auria, I. V. Elkin, and O. I. Melikhov, "Investigation of accident management procedures related to loss of feedwater and station blackout in PSB-VVER integral test facility," *Nuclear Engineering and Design*, vol. 250, pp. 633–645, 2012.

[10] K. Umminger, L. Dennhardt, S. Schollenberger, and B. Schoen, "Integral test facility PKL: experimental PWR accident investigation," *Science and Technology of Nuclear Installations*, vol. 2012, Article ID 891056, 16 pages, 2012.

[11] T. Takeda and I. Ohtsu, "ROSA/LSTF experiment on a PWR station blackout transient with accident management measures and RELAP5 analyses," *Mechanical Engineering Journal*, vol. 2, no. 5, pp. 15-00132–15-00132, 2015.

[12] K. Yoshihara, "Current situation of safety assurance measures in the light of fukushima: Daiichi accident taken by kansai electric power Co., Inc.," *Atomos*, vol. 54, no. 7, pp. 441–446, 2012.

[13] T. Takeda, A. Ohwada, and H. Nakamura, "Measurement of non-condensable gas in a PWR small-break LOCA simulation test with LSTF for OECD/NEA ROSA Project and RELAP5 post-test analysis," *Experimental Thermal and Fluid Science*, vol. 51, pp. 112–121, 2013.

[14] T. Takeda, "RELAP5 Analyses of ROSA/LSTF Experiments on AM Measures during PWR Vessel Bottom Small-Break LOCAs with Gas Inflow," *International Journal of Nuclear Energy*, vol. 2014, Article ID 803470, 17 pages, 2014.

[15] T. Takeda and I. Ohtsu, "ROSA/LSTF experiment on accident management measures during a PWR station blackout transient with pump seal leakage and RELAP5 analyses," *Journal of Energy and Power Sources*, vol. 2, no. 7, pp. 274–290, 2015.

[16] T. Watanabe and Y. Kukita, "Experiment and analyses of PWR station blackout transient involving pump seal leak in," in *Proceedings of the 6th International Topical Meeting on Nuclear Reactor Thermal Hydraulics (NURETH-6)*, Grenoble, France, October 1993.

[17] The ROSA-V Group, *ROSA-V Large Scale Test Facility (LSTF) System Description for The Third And Fourth Simulated Fuel Assemblies," JAERI-Tech 2003-037*, Japan Atomic Energy Research Institute, Ibaraki, Japan, 2003.

[18] USNRC Nuclear Safety Analysis Division, "RELAP5/MOD3.3 code manual," Tech. Rep. NUREG/CR-5535/Rev 1, Information Systems Laboratories, Inc., 2001.

[19] N. Zuber, "Problems in modeling small break LOCA," Tech. Rep. USNRC Report NUREG-0724, 1980.

[20] H. Kumamaru and K. Tasaka, "Recalculation of simulated post-scram core power decay curve for use in ROSA-IV/LSTF experiments on PWR small-break LOCAs and transients," Tech. Rep., Japan Atomic Energy Research Institute, Ibaraki, Japan, 1990.

[21] H. Asaka, Y. Kukita, T. Yonomoto, Y. Koizumi, and K. Tasaka, "Results of 0.5% cold-leg small-break LOCA experiments at ROSA-IV/LSTF: effect of break orientation," *Experimental Thermal and Fluid Science*, vol. 3, no. 6, pp. 588–596, 1990.

[22] H. K. Fauske, "The discharge of saturated water through tubes," *Chemical Engineering and Progress Symposium Series*, vol. 61, no. 59, pp. 210–216, 1965.

[23] K. H. Ardron and R. A. Furness, "A study of the critical flow models used in reactor blowdown analysis," *Nuclear Engineering and Design*, vol. 39, no. 2-3, pp. 257–266, 1976.

[24] D. W. Sallet, "Thermal hydraulics of valves for nuclear applications," *Nuclear Science and Engineering*, vol. 88, no. 3, pp. 220–244, 1984.

[25] S. Susyadi and T. Yonomoto, "Analysis on non uniform flow in steam generator during steady state natural circulation cooling," JAERI-Research 2005-011, Japan Atomic Energy Research Institute, Ibaraki, Japan, 2005.

[26] T. Takeda, H. Asaka, and H. Nakamura, "RELAP5 analysis of OECD/NEA ROSA project experiment simulating a PWR loss-of-feedwater transient with high-power natural circulation," *Science and Technology of Nuclear Installations*, vol. 2012, Article ID 957285, 15 pages, 2012.

[27] M. M. Shah, "A general correlation for heat transfer during film condensation inside pipes," *International Journal of Heat and Mass Transfer*, vol. 22, no. 4, pp. 547–556, 1979.

[28] W. A. Nusselt, "The surface condensation of water vapor," *Zeitschrift des Vereines Deutscher Ingenieure*, vol. 60, pp. 541–546, 1916.

[29] K. M. Vierow and V. E. Schrock, "Condensation in a natural circulation loop with non-condensable gases part Iheat transfer," in *Proceedings of the International Conference on Multiphase Flows*, Ibaraki, Japan, September 1991.

[30] A. Prošek, *RELAP5 and TRACE calculations of LOCA in PWR," NUREG/IA-0479 International Agreement Report*, U.S. Nuclear Regulatory Commission, Washington DC, Wash, USA, 2017.